Journal of Catalysis 272 (2010) 151–157

Contents lists available at ScienceDirect

Journal of Catalysis

journal homepage: www.elsevier.com/locate/jcat

A density functional theory study of water gas shift over pseudomorphic monolayer alloy catalysts: Comparison with NO oxidation

Jelena Jelic, Randall J. Meyer *

Department of Chemical Engineering, University of Illinois at Chicago, 810 S Clinton, Chicago, IL 60607-7000, United States

ARTICLE INFO

Article history:
Received 18 November 2009
Revised 28 February 2010
Accepted 2 March 2010
Available online 13 April 2010

Keywords:
Platinum
Alloy
Catalyst
WGS
NSR
Density functional theory
NO_x
Pseudomorphic

ABSTRACT

The water gas shift reaction has been studied with density functional theory on Pt(1 1 1)/M(1 1 1) pseudomorphic monolayer catalysts (where M is the host metal). Both redox and carboxyl intermediate mechanisms were explored. It was found that the barriers for dissociation reactions (H_2O, OH, OH disproportionation) are lower on systems with an expanded lattice parameter of Pt (when compared to pure Pt) and that the barriers for formation reactions (CO oxidation, carboxyl formation) are higher compared to Pt(1 1 1). Similarly, this situation is reversed for the alloys with a compressed lattice parameter. In all cases, the carboxyl reaction path is favored and water dissociation was found to have the highest barrier along the reaction path. Using results from our previous studies for NO oxidation for NO_x storage reduction (NSR) on the same systems, we were able to construct volcano plots for both the oxidation mode and the reduction mode of NSR (if H_2 produced from WGS is conceived to be kinetically critical).

© 2010 Elsevier Inc. All rights reserved.

1. Introduction

The water gas shift (WGS) reaction is an important reaction for the generation of high-purity hydrogen while converting carbon monoxide. The reaction is slightly exothermic at room temperature, yielding 42 kJ per mole. Therefore, while low reaction temperatures push the equilibrium toward hydrogen production, higher temperatures are often desirable to increase the reaction rates. Copper-based WGS catalysts are currently the industry standard [1–3]. However, recent work from Mavrikakis and Dumesic has shown that Cu/Pt near-surface alloys are potentially superior to pure transition metals for low-temperature WGS catalyst [4]. Therefore, it is interesting to consider what other types of near-surface alloys may be of interest and could been seen as potential competitors to copper-based systems.

In addition to systems where water gas shift is the primary reaction, water gas shift also occurs as a side reaction in many processes of high importance (e.g., steam reforming of methane [5]). In fact, water gas shift must be considered in any system in which water and carbon monoxide are present. Of course, one such system is in the catalytic convertor of automotive vehicles (or for that matter any hydrocarbon combustion process) where incomplete combustion can result in the presence of carbon monoxide. Therefore, in addition to the complicated chemistry of NO_x reduction, one must remember that any water present may react with CO to produce hydrogen that may be available for reaction with other surface species [6–10]. Of particular interest is the presence of water gas shift (or reverse water gas shift) in lean NO_x reduction where carbon monoxide may be present as a reductant and may react with water to produce hydrogen or conversely hydrogen present as a reductant may be consumed by CO_2 to produce CO depending on the temperature and partial pressures of relevant species.

One strategy for lean NO_x reduction is the use of lean NO_x traps or NO_x storage reduction (NSR) systems. First pioneered by researchers at Toyota [8,11–14], the NO_x storage catalyst system operates under cycling conditions. First, NO reacts with oxygen over a noble metal (usually Pt) to form NO_2, which can subsequently adsorb on a storage material (usually BaO, forming barium nitrate) until the storage material is fully loaded. Then, the reaction condition is abruptly changed with an injection of a reducing agent. The reducing agent reacts with NO_x over the Pt catalyst (or at the catalyst/storage material interface) producing the typical exhaust products: N_2, H_2O, and CO_2 (depending upon the reductant). Many choices exist for the reductant in this scheme including hydrogen, hydrocarbons, ammonia, and CO [15–17]. In the current study, we will examine WGS in the context of the use of CO as a reductant. CO may react directly with stored NO_x (in the absence of H_2O to produce NCO) [18–21], but it may also act as a source

* Corresponding author.
E-mail address: rjm@uic.edu (R.J. Meyer).

0021-9517/$ - see front matter © 2010 Elsevier Inc. All rights reserved.
doi:10.1016/j.jcat.2010.03.002

of hydrogen by way of the water gas shift reaction [20–23]. Therefore, an ideal NO_x reduction catalyst must also function as a WGS catalyst.

Surface science studies of epitaxially grown metal layers on top of a different metal single crystal have revealed that these pseudomorphic monolayers have novel adsorption properties and therefore could potentially serve as a whole new class of catalysts [24–30]. A combination of ligand and strain effects perturbs the electronic structure of the surface layer and therefore the catalytic properties of these alloy systems may be vastly different than either of its pure metal components. We have previously exploited this phenomenon to examine how the electronic structure of Pt and Pd pseudomorphic alloy systems are related to their ability to catalyze NO oxidation [31]. A volcano plot of NO oxidation was created that showed that for systems in expansion that have their *d*-band centers shifted toward the Fermi level (e.g., Pd over Au(1 1 1)), the slowest step in NO oxidation is the reaction between adsorbed NO and adsorbed O atoms (given a coverage of 0.25 ML of each reactant). However, for systems in compression whose *d*-band center has been pushed away from the Fermi level, O_2 dissociation now has a higher barrier. In our current studies, we explore Pt-based pseudomorphic monolayer catalysts for their ability to perform water gas shift. It is intended that a similar volcano plot can be constructed for WGS and used together with the volcano plot for NO oxidation to describe a catalyst that will be sufficiently active for both NO oxidation and water gas shift.

2. Methodology

The calculations in this work are performed using the Vienna Ab Initio Simulation Package (VASP) [32,33] that is based on density functional theory (DFT) and uses a plane-wave basis set with plane-wave cut of energy $E_{cut} = 400$ eV and ultrasoft Vanderbilt pseudopotentials [34]. We used the Perdew Wang (PW-91) form of the exchange and correlation functional within the generalized gradient approximation (GGA) [35]. The Brillouin zone is sampled with a uniform dense $9 \times 9 \times 1$ k-point grid (Monkhorst Pack) [36].

The slab representing the system consists of (2×2) three monolayers of close-packed (1 1 1) fcc metals (Rh, Ir, Pd, Au, Ag) or (0 0 0 1) hcp Ru with a single Pt monolayer above the host metal. The two uppermost metal layers are allowed to relax. Approximately five layers of vacuum were used to separate the slabs.

Reaction paths and barriers are determined using the Climbing Nudged Elastic Band (NEB) method [37]. In the NEB method, a reaction coordinate relating the initial and final states is defined and a set of intermediate states are distributed along the reaction path. Each intermediate state is fully relaxed in the hyperspace perpendicular to the reaction coordinate. Vibrational frequencies were computed for the initial, transition, and final states, where the substrate is frozen but adsorbates are allowed to vibrate in any direction. If the molecule is in a true transition state, it should have one and only one imaginary frequency.

3. Results and discussion

The water gas shift reaction has been extensively studied, and at least two competing reaction mechanisms have been proposed [38–44]. One is a redox mechanism where water is completely dissociated to hydrogen and oxygen atoms (usually involving participation of oxygen vacancies at the metal/support interface [45]) before CO reacts with an oxygen atom to form CO_2. An alternative mechanism, sometimes called an associative mechanism, where CO reacts with hydroxyl groups to form carboxyl or formate [46–48] as reaction intermediates, is also viable in many systems. We will consider both possibilities in this work (but in the absence of participation of the support) and examine the effect of electronic structure on the barriers of individual steps in water gas shift.

3.1. Redox mechanism

The redox mechanism described above can be presented in elementary steps as follows (where * refers to an empty surface site and X^* refers to species X on the surface):

$$CO + {}^* \leftrightarrow CO^* \quad (1)$$

$$H_2O + {}^* \leftrightarrow H_2O^* \quad (2)$$

$$H_2O^* + {}^* \leftrightarrow OH^* + H^* \quad (3)$$

$$OH^* + {}^* \leftrightarrow O^* + H^* \quad (4)$$

$$OH^* + OH^* \leftrightarrow H_2O^* + O^* \quad (5)$$

$$CO^* + O^* \leftrightarrow CO_2^* + {}^* \quad (6)$$

$$CO_2^* \leftrightarrow CO_2 + {}^* \quad (7)$$

$$H^* + H^* \leftrightarrow H_2 + 2^* \quad (8)$$

In this mechanism, carbon monoxide and water are adsorbed onto the surface. Water may dissociate to a hydrogen atom and a hydroxyl group. The hydroxyl group can then further dissociate into atomic hydrogen and atomic oxygen. Alternatively, atomic oxygen may be produced by hydroxyl disproportionation (step 5). CO and atomic oxygen can then react to produce CO_2, which rapidly desorbs from the surface.

Mavrikakis et al. have fully calculated the redox mechanism for WGS on Pt(1 1 1) and we reproduce their results with minimal changes as a basis for our examination [49]. On Pt(1 1 1), CO prefers to adsorb onto an fcc 3-fold hollow site and binding energy is −1.83 eV (this is the common GGA over-coordination error but does not affect the results presented here [50]). H_2O adsorbs only weakly in an atop configuration parallel to the surface. In Table 1, the adsorption energies for CO and H_2O on all Pt pseudomorphic monolayer alloys considered are given. The order of elements is due to position of the *d*-band center of Pt atoms at top layer.

When the Au is a host metal, the center of the Pt *d*-band energy levels is closest to the Fermi level and when Ir is host metal, the center of the Pt *d*-band is furthest from the Fermi level. As expected following the *d*-band model of Norskov and coworkers [51,52], Pt above Au is the most reactive pseudomorphic monolayer alloy for CO adsorption and we can see a clear trend of the adsorption energies. In contrast, water, which adsorbs weakly on Pt(1 1 1), is not sensitive to the changes in electronic structure. This is a consequence of the combination of the preferred binding site for water (atop that has lower coordination to the surface) and the weak binding of water on all surfaces considered.

After adsorption on the surface, water may dissociate to atomic hydrogen and a hydroxyl group. The barrier for water dissociation on Pt(1 1 1) is found to be 0.96 eV and the reaction enthalpy is 0.77 eV. The preferred adsorption site for hydroxyl group is an atop site with a tilt. After dissociation, hydrogen goes to the atop site (on Pt(1 1 1) binding energy is −0.39 eV, referenced to gas phase H_2) but can move easily to the fcc 3-fold site (−0.47 eV binding energy on Pt(1 1 1)). The same adsorption sites are preferred for all Pt pseudomorphic monolayer systems.

Brønsted–Evans–Polanyi (BEP) relationships [53–57] are empirically established phenomena that state that there is a linear

Table 1
Binding energies of CO on Pt pseudomorphic monolayer alloys. The elements indicate the host metal, the surface metal is always Pt.

Host metal	Au	Ag	Pd	Pt	Rh	Ru	Ir
d-band center	−6.34	−6.70	−6.80	−6.93	−6.99	−7.23	−7.50
E_{ads} for CO	−2.07	−2.04	−1.85	−1.83	−1.34	−1.04	−1.25
E_{ads} for H_2O	−0.32	−0.34	−0.30	−0.30	−0.24	−0.24	−0.28

relationship between the activation energy and the reaction enthalpy for an elementary reaction on the surface of the catalyst. This relation is independent of the reactant and of the metal but is subject to the structure of the active site and the transition state.

$$E_{act.} = A + B \cdot \Delta H$$

BEP relationships have been useful in understanding the connection between classes of reactions (e.g., diatomic dissociation) for a number of simple cases. For water dissociation on pseudomorphic monolayer systems, a BEP plot is shown in Fig. 1.

For all the Pt pseudomorphic monolayer systems, the adsorption energy of water is found to be almost equal regardless of the substrate (as given in Table 1). However, the adsorption energy of atomic hydrogen (and for hydroxyl) is larger for systems with expanded lattice parameters (i.e., Pt over Au and Ag) than for Pt(1 1 1). As a result, the dissociation of water over Pt above Au and Ag is less endothermic than that for Pt(1 1 1) and the reaction barriers are smaller. Conversely, the adsorption of atomic hydrogen and hydroxyl is weaker on Pt monolayers in compression and so water dissociation is even more endothermic than on Pt(1 1 1).

After water dissociation, the hydroxyl group, initially located at the atop-tilted site, may move to a bridge site. It then can dissociate to hydrogen and atomic oxygen. On Pt(1 1 1), hydroxyl dissociation is endothermic with a reaction enthalpy of 0.22 eV and a barrier of 1.08 eV. The BEP plot for hydroxyl dissociation is shown in Fig. 2. Once again, a trend is observed as the surfaces with the Pt layer in expansion have lower barriers when compared to surfaces where the monolayer of Pt is in compression.

The slopes of the BEP relationships for both water dissociation and hydroxyl dissociation are close to unity. This implies that both reactions have product-like or "late" transition states [54]. On the other hand, the intercepts of the BEP plots for these two reactions are different as the intercept is much higher for OH dissociation (1.00 eV as opposed to 0.21 eV). According to Michaelides et al. [55], if the slope is equal to one, then the intercept can be interpreted as the activation energy of the reverse reaction, suggesting that OH hydrogenation is significantly easier than O hydrogenation. We can rationalize this result as products of OH dissociation reaction are even more strongly bound to the surface when compared to the products of H_2O dissociation and accordingly, the intercept of BEP plot is higher.

Complete water dissociation provides the atomic oxygen necessary for CO oxidation, but the barrier for OH dissociation is even higher than for H_2O dissociation. However, another way of obtaining atomic oxygen on the surface is through OH disproportionation (step 5). On Pt(1 1 1), the hydroxyl disproportionation reaction exothermic with a reaction enthalpy of −0.34 eV and has a low barrier of only 0.28 eV. The BEP plot for the OH disproportionation reaction is shown in Fig. 3. Barriers for all the systems considered are low, implying that this way of providing atomic oxygen for CO oxidation is much more favorable than OH dissociation. Recent work from Schneider and coworkers [58] has shown that OH coverage dominates the surface compared to atomic oxygen in water gas shift for a variety of metal surfaces so it is not inconceivable that OH disproportionation is the dominant path to atomic oxygen production.

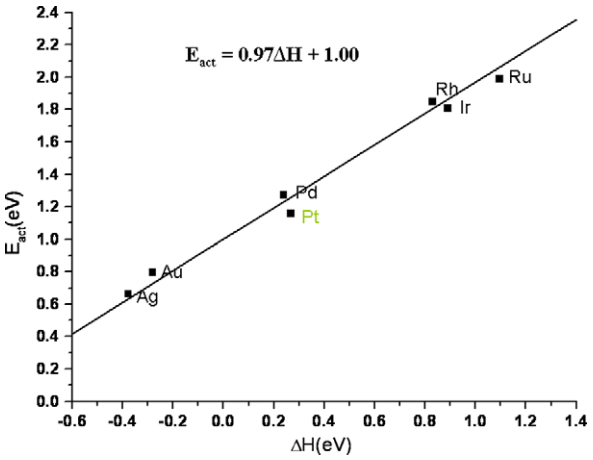

Fig. 2. BEP plot for OH dissociation on Pt pseudomorphic monolayer systems. The elements indicate the host metal, the surface metal is always Pt.

When oxygen is present on the surface, CO changes its preferred adsorption site from the fcc site to the atop site. For Pt(1 1 1), the energy gain from changing the adsorption site is 0.27 eV. CO oxidation on Pt(1 1 1) is exothermic with a reaction enthalpy of −0.77 eV and the barrier for the reaction is 1.00 eV. The BEP plot for CO oxidation over Pt pseudomorphic monolayer systems is depicted in Fig. 4. The trend for CO oxidation is opposite that of H_2O and OH dissociation. The difference in the binding energy of CO_2 between Pt pseudomorphic monolayer alloys is small (not shown but similar to H_2O), but both oxygen atoms and CO adsorb much more strongly on Pt pseudomorphic monolayers above Au and Ag than on Pt(1 1 1) and somewhat weaker on Pt above the other metals considered.

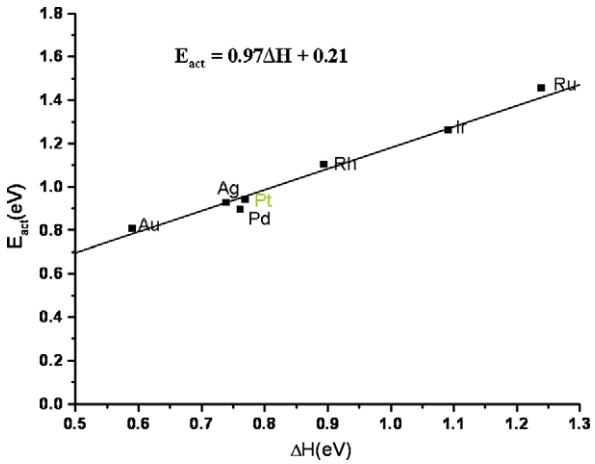

Fig. 1. BEP plot for water dissociation on Pt pseudomorphic monolayer systems. The elements indicate the host metal, the surface metal is always Pt.

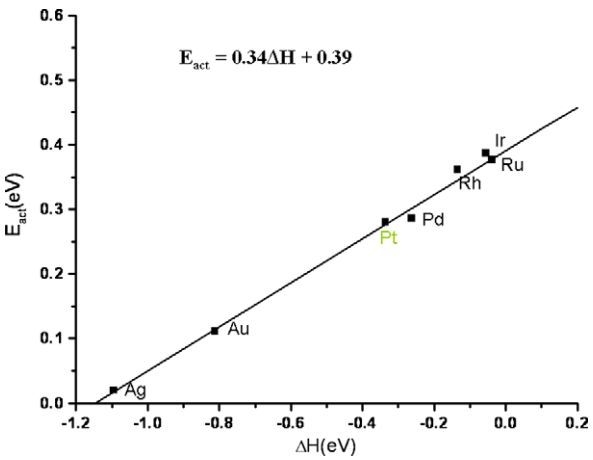

Fig. 3. BEP plot for OH disproportionation on Pt pseudomorphic monolayer systems. The elements indicate the host metal, the surface metal is always Pt.

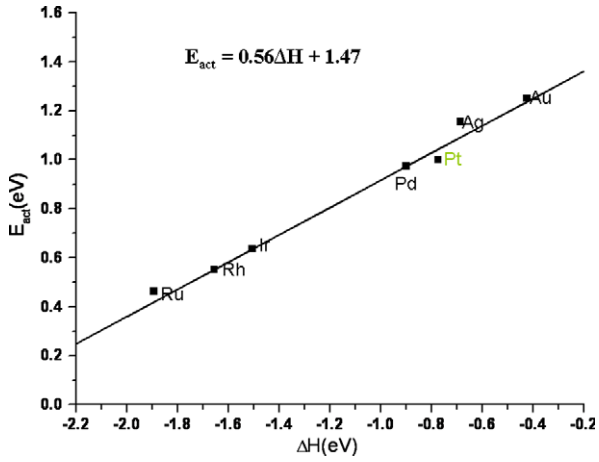

Fig. 4. BEP plot for CO oxidation on pseudomorphic monolayer system. The elements indicate the host metal, the surface metal is always Pt.

In the redox mechanism, H_2O dissociation, OH dissociation, and CO oxidation reactions all have high barriers and therefore all of these steps may be kinetically important. For H_2O and OH dissociation, systems with compressed lattice parameters (Pt over Rh, Ru and Ir) have a higher barriers than systems with expanded lattice parameters. However, for CO oxidation, the trend reverses, and systems with expanded lattice parameters have higher barriers (Pt over Au and Ag and for these systems, CO oxidation is rate-limiting step). For both Pt(1 1 1) and Pt over Pd, barriers for water dissociation and CO oxidation are very similar, implying both steps will contribute to the kinetics (we have not performed a full sensitivity analysis to determine the degree of rate control) [49,59]. It is important to recognize that we have performed all our calculations at a coverage of 0.25 ML. It should be noted that under typical reaction conditions, the CO coverage is usually higher than water so the effect of coverage will shift barriers in favor for CO oxidation [60]. As coverage increases, the barrier for water dissociation will increase and the barrier for CO oxidation will decrease, so the volcano plot that we could develop here will necessarily shift with partial pressure and temperature as coverages shift.

3.2. Carboxyl mechanism

In the carboxyl mechanism, OH, rather than atomic oxygen, is the primary oxidant for CO_2 production. A hydroxyl group may react with CO and form two possible intermediates: carboxyl (HOCO or sometimes written as COOH) or formate (HCOO) depicted in Fig. 5. Experimental studies on Pt catalysts have shown that formate could be the possible intermediate [43,44] but formate formation from CO and OH involves either insertion of CO into an O–H bond (an extremely energetic process) or the breaking of the OH bond followed by hydrogenation of CO to form HCO and then addition of oxygen to HCO [40]. In their DFT examination of WGS over Au catalysts, Hu et al. found that the reaction of OH and CO to form HCO had a barrier of 1.8 eV and a reaction enthalpy of 0.8 eV. In their DFT evaluation of WGS over Pt(1 1 1), Mavrikakis and coworkers [49] proposed that formyl could also be formed from a reaction of carboxyl with CO. However, this reaction also was found to be highly endothermic (0.83 eV) and the barrier was not calculated. In addition, Mavrikakis et al. showed that further decomposition of formate into CO_2 and hydrogen has higher barrier (1.04 eV) than carboxyl decomposition (0.78 eV). Furthermore, there exists some evidence for the reaction of CO and OH to form carboxyl, as the presence of coadsorbed water greatly enhanced CO oxidation on Pt(1 1 1) [61]. Most recently, Rodriguez and co-workers have used a combination of IRAS and NEXAFS to investigate the presence of reaction intermediates in WGS on Au(1 1 1) [41]. In their work, Rodriguez et al. observed that coadsorbed OH and CO reacted rapidly between 90 and 120 K, consistent with the presence of an unstable HOCO intermediate (in contrast, formate is stable up to 350 K). Therefore, we only consider carboxyl routes in this work.

$$CO^* + OH^* \leftrightarrow HOCO^* + {}^* \quad (9)$$

$$HOCO^* + {}^* \leftrightarrow CO_2^* + H^* \quad (10)$$

When CO and OH are present on the surface, CO does not change its preferred adsorption site, and remains in fcc 3-fold hollow site (again, this is a product of the GGA over-coordination problem). On Pt(1 1 1), the carboxyl formation reaction is exothermic with a reaction enthalpy of −0.37 eV and has a barrier of 0.56 eV. When we compare this result to CO_2 production through CO oxidation with atomic oxygen, the carboxyl reaction is less exothermic, but the barrier is considerably smaller. The BEP plot for carboxyl formation is given in Fig. 6. If we compare Figs. 4 and 6 for the case of Pt over Au and Ag, the barrier is still much smaller for HOCO formation than for CO oxidation.

Barriers for carboxyl formation are not just smaller than barriers to CO oxidation with oxygen atoms, but the highest barrier for carboxyl formation is also smaller than smallest barrier for water dissociation. CO_2 will be produced when HOCO dissociates into CO_2 and a hydrogen atom as indicated in reaction 10. However, before that can occur, HOCO must change its orientation such that the OH bond points toward the surface (in Fig. 5b) as opposed to away from the surface (as indicated in Fig. 5a). The barrier for rotation of the hydrogen for carboxyl bound to Pt(1 1 1) has been found to be 0.32 eV. We have not calculated this for every surface since the barrier is not likely to be sensitive to the identity of the surface as neither O nor H is bound to the substrate. After rotation of the hydrogen, the O–H bond can be cleaved (as well as the surface-C bond) to result in gas phase CO_2 and surface bound H.

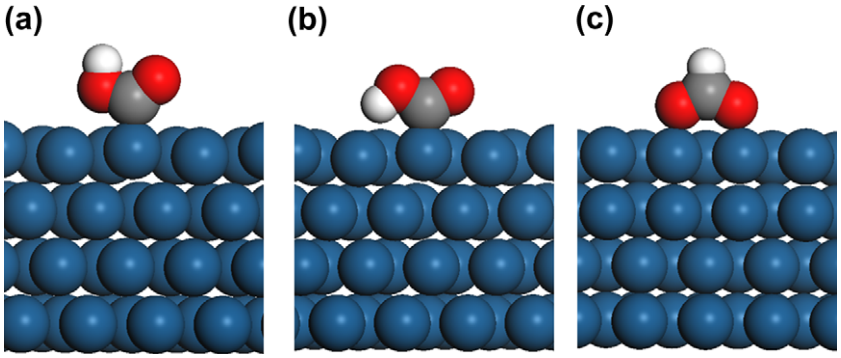

Fig. 5. Side view of two carboxyl (COOH) structures: (a) cis-COOH, (b) trans-COOH and formate (HCOO) structure, and (c) bidentate-HCOO.

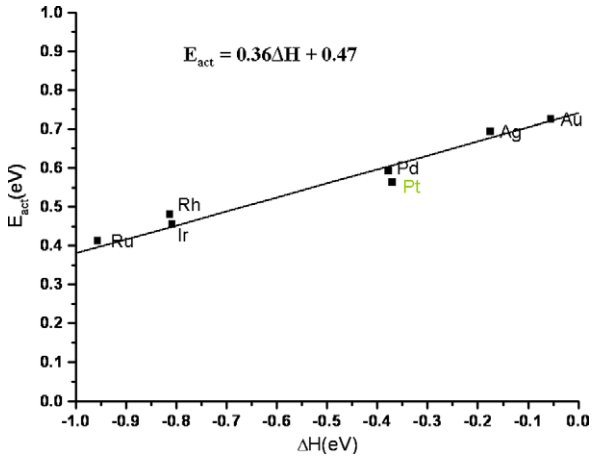

Fig. 6. BEP plot for HOCO formation on Pt pseudomorphic monolayer systems. The elements indicate the host metal, the surface metal is always Pt.

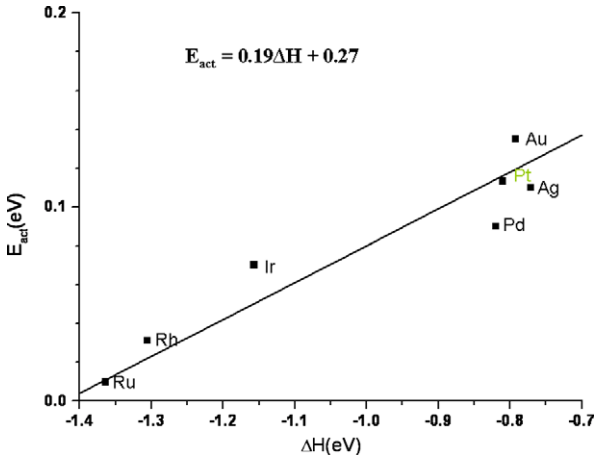

Fig. 8. BEP plot for reaction of HOCO and OH on Pt pseudomorphic monolayer systems. The elements indicate the host metal, the surface metal is always Pt.

Reaction enthalpies and barriers for carboxyl decomposition are presented in Fig. 7.

Reaction enthalpies do not vary significantly between the Pt pseudomorphic monolayer systems. Barriers for carboxyl decomposition have the same trend as for CO oxidation as the barrier to carboxyl decomposition is primarily controlled by the strength of the surface-C bond. Therefore, barriers for carboxyl decomposition are highest for the systems with expanded lattice parameters. Once again, except for systems of Pt above Au or Ag, water dissociation possesses the highest barrier and will be considered the rate-limiting step in the water gas shift reaction.

Finally, there is an additional alternative route to carboxyl decomposition through reaction of HOCO with OH on the surface to produce water and CO_2. Just as in the case of hydroxyl disproportionation to produce water and oxygen atoms, the reaction with hydroxyl has a very low barrier on Pt(1 1 1) (0.12 eV) and could be conceived as a viable pathway to carboxyl decomposition. The complete BEP plot for this reaction is shown in Fig. 8. In many cases, the barriers are too low to be considered to be true transition states and one may assume that the reaction is spontaneous. In recent work from Schneider et al., a thermodynamic analysis of water dissociation over a variety of metal surfaces shows that the surface is likely to be dominated by hydrogen [58]. However, there may be sufficient hydroxyl density to react with HOCO to form CO_2 and water, thus providing another route to CO_2.

NSR catalysts work in two distinct modes: oxidation and reduction. Previously, we have examined NO oxidation reaction as well as oxygen dissociation on Pt pseudomorphic monolayer alloy systems [31]. We have constructed a volcano plot based upon NO oxidation and found that for 0.25 ML of NO and O, NO oxidation was found to possess a higher barrier than O_2 dissociation for almost all systems. In this study, we have calculated barriers for WGS reaction, since in reduction mode this reaction will be one of the sources of the hydrogen for reduction chemistry. Although any step in WGS is not likely controlling the overall kinetics of NO_x reduction during the rich cycle in NSR [23,62,63], we have chosen this as a model system to demonstrate the interplay of the volcano plots for the two systems. For the WGS reaction on pseudomorphic monolayer systems, we find water dissociation as the step with the highest barrier (naively without detailed kinetic analysis, one could term this rate limiting) on most of the systems. As a combined result for whole NSR catalyst, we present volcano plots in Fig. 9 for NO oxidation and water gas shift on all studied Pt pseudomorphic monolayer systems. In Fig. 9, we have evaluated the rate assuming an Arrhenius expression given an arbitrary pre-exponential, choosing a reaction temperature of 600 K and using the highest barrier in the process as the activation energy. We have then normalized this estimated reaction rate based upon the rate

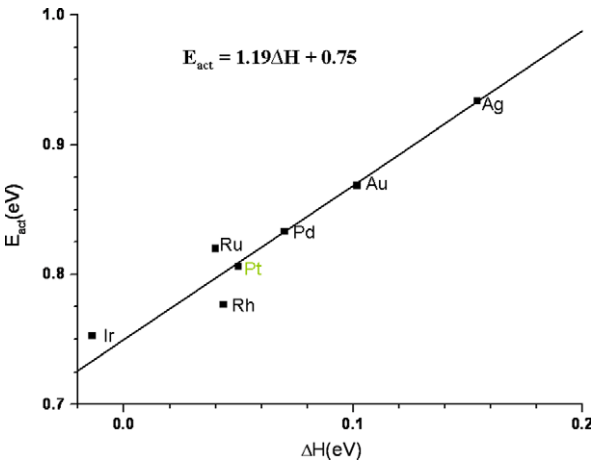

Fig. 7. BEP plot for HOCO decomposition on Pt pseudomorphic monolayer systems. The elements indicate the host metal, the surface metal is always Pt.

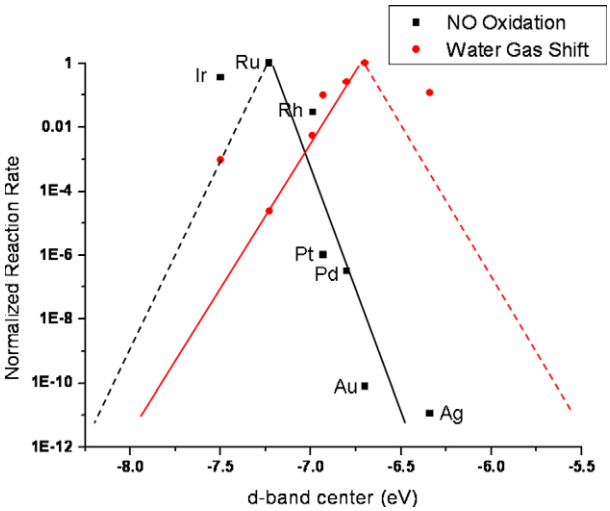

Fig. 9. Volcano plots for the NO oxidation and water gas shift reactions. The elements indicate the host metal, the surface metal is always Pt.

for the most active catalyst assuming that the rate is based solely on the slow step in the process for all catalysts. Therefore, for the case of NO oxidation, we have calculated a rate based upon either the NO + O reaction or O_2 dissociation depending upon which reaction has the highest barrier for a particular pseudomorphic monolayer system. Similarly, we have repeated this process for the WGS shift reaction. In all cases, the carboxyl pathway will be favored over the redox pathway. Water dissociation was found to be the slowest step in every case except Pt/Ag(1 1 1) in which case carboxyl decomposition to CO_2 and hydrogen was found to have the highest barrier. The two reactions have opposite trends as the rates for the NO oxidation reaction on the systems with compressed Pt lattice parameters are high because binding energies of the reactants is lower for these systems (not unsurprising for an association reaction). At the same time, the rates for WGS are lower as the barriers for water dissociation are higher for these systems compared to those with expanded lattice parameter. What is important to notice is that the rates for the water dissociation do not drop significantly on the systems with compressed lattice parameter in contrast to the severe decline in the rates for NO oxidation for the systems with expanded lattice parameters. Overlaying the two volcano plots, one can suggest candidate alloys that should have reasonable performance for both reaction modes. Based on our simple analysis of the reduction chemistry, Pt over Rh would represent the best candidate for both working regimes. Although we have not made judgments about the relative importance of the NO oxidation and WGS shift reaction for the overall performance of the NSR catalyst system, our work suggests a strategy that may be employed to take on this unique system that requires operation in two distinct regimes.

It should be noted that these catalysts may not be stable in the WGS reaction environment. We have not performed an extensive analysis of their stability for WGS. However, it can be reasoned that adsorption of H_2O and CO is not likely to disrupt the segregated structure of the pseudomorphic monolayer systems in any case in which O does not as the adsorption of oxygen atoms is stronger than any intermediate involved in the WGS reaction. Therefore, based upon our previous investigation [31], we can conclude that the Pt/Rh system should be stable at low temperature in the WGS environment.

4. Conclusion

DFT calculations were performed to calculate reaction enthalpies and barriers for elementary steps in WGS reaction on Pt-based pseudomorphic monolayer systems. Both redox and carboxyl mechanisms were examined. On Pt(1 1 1), for 0.25 ML coverage, water dissociation has a slightly lower barrier than CO oxidation. The carboxyl mechanism is therefore favored over the redox mechanism in all cases. Expansion of Pt lattice by placing it above Au or Ag will increase the adsorption energy of the products of water dissociation and lower the barrier for the water dissociation reaction. In contrast, placing Pt above metals with smaller lattice parameter (Ru, Rh, Ir) will increase the barrier for water dissociation (but decrease barrier for CO and NO oxidation). Our approach, although simplistic, outlines a strategy for optimization by overlaying volcano plots for both the oxidation reaction and the reduction side chemistry of the NSR cycle as the ideal catalyst must be able to perform in two distinct environments.

Acknowledgments

We gratefully acknowledge funding for this work from the National Science Foundation (CBET Grant #0730937). We gratefully acknowledge NCSA for allocation Grant #CTS 070044T that was used to perform some of the calculations described herein. Finally, we wish to thank the organizers of the CAMD-PIRE workshop for training and support for this work through the National Science Foundation Grant OISE #0730277.

References

[1] C.V. Ovesen, P. Stoltze, J.K. Norskov, C.T. Campbell, J. Catal. 134 (1992) 445–468.
[2] C.V. Ovesen, B.S. Clausen, B.S. Hammershoi, G. Steffensen, T. Askgaard, I. Chorkendorff, J.K. Norskov, P.B. Rasmussen, P. Stoltze, P. Taylor, J. Catal. 158 (1996) 170–180.
[3] J.A. Rodriguez, P. Liu, X. Wang, W. Wen, J. Hanson, J. Hrbek, M. Perez, J. Evans, Catal. Today 143 (2009) 45–50.
[4] J. Knudsen, A.U. Nilekar, R.T. Vang, J. Schnadt, E.L. Kunkes, J.A. Dumesic, M. Mavrikakis, F. Besenbacher, J. Am. Chem. Soc. 129 (2007) 6485–6490.
[5] J.R. Rostrup-Nielsen, J. Sehested, J.K. Norskov, Adv. Catal. 47 (47) (2002) 65–139.
[6] Y.J. Li, S. Roth, J. Dettling, T. Beutel, Top. Catal. 16 (2001) 139–144.
[7] L. Lietti, P. Forzatti, I. Nova, E. Tronconi, J. Catal. 204 (2001) 175–191.
[8] W.S. Epling, L.E. Campbell, A. Yezerets, N.W. Currier, J.E. Parks, Catal. Rev. Sci. Eng. 46 (2004) 163–245.
[9] J. Xu, M.P. Harold, V. Balakotaiah, Appl. Catal. B – Environ. 89 (2009) 73–86.
[10] P. Forzatti, L. Castoldi, I. Nova, L. Lietti, E. Tronconi, Catal. Today 117 (2006) 316–320.
[11] S. Matsumoto, CATTECH 4 (2002) 102–109.
[12] M. Takeuchi, S. Matsumoto, Top. Catal. 28 (2004) 151–156.
[13] N. Takahashi, H. Shinjoh, T. Iijima, T. Suzuki, K. Yamazaki, K. Yokota, H. Suzuki, N. Miyoshi, S. Matsumoto, T. Tanizawa, T. Tanaka, S. Tateishi, K. Kasahara, Catal. Today 27 (1996) 63–69.
[14] S. Matsumoto, Catal. Today 29 (1996) 43–45.
[15] H. Abdulhamid, E. Fridell, M. Skoglundh, Top. Catal. 30–31 (2004) 161–168.
[16] L. Cumaranatunge, S.S. Mulla, A. Yezerets, N.W. Currier, W.N. Delgass, F.H. Ribeiro, J. Catal. 246 (2007) 29–34.
[17] T. Szailer, J.H. Kwak, D.H. Kim, J.C. Hanson, C.H.F. Peden, J. Szanyi, J. Catal. 239 (2006) 51–64.
[18] Z.Q. Liu, J.A. Anderson, J. Catal. 224 (2004) 18–27.
[19] T. Lesage, C. Verrier, P. Bazin, J. Saussey, M. Daturi, Phys. Chem. Chem. Phys. 5 (2003) 4435–4440.
[20] I. Nova, L. Lietti, P. Forzatti, F. Frola, F. Prinetto, G. Ghiotti, Top. Catal. 52 (2009) 1757–1761.
[21] M. Al-Harbi, W.S. Epling, Appl. Catal. B – Environ. 89 (2009) 315–325.
[22] J.S. Choi, W.P. Partridge, C.S. Daw, Appl. Catal. A 293 (2005) 24–40.
[23] C.M.L. Scholz, K.M. Nauta, M.H.J.M. de Croon, J.C. Schouten, Chem. Eng. Sci. 63 (2008) 2843–2855.
[24] J.L. Zhang, M.B. Vukmirovic, Y. Xu, M. Mavrikakis, R.R. Adzic, Angew Chem. Int. Ed. 44 (2005) 2132–2135.
[25] T. Jirsak, J. Dvorak, J.A. Rodriguez, Surf. Sci. 436 (1999) L683–L690.
[26] D.E. Beck, J.M. Heitzinger, A. Avoyan, B.E. Koel, Surf. Sci. 491 (2001) 48–62.
[27] P. Dolle, R. Baudoing-Savois, M. De Santis, M.C. Saint-Lager, M. Abel, J.C. Bertolini, P. Delichere, Surf. Sci. 518 (2002) 1–13.
[28] J.A. Rodriguez, Surf. Sci. Rep. 24 (1996) 225–287.
[29] J. Greeley, M. Mavrikakis, Nat. Mater. 3 (2004) 810–815.
[30] M.B. Zellner, A.M. Goda, O. Skoplyak, M.A. Barteau, J.G. Chen, Surf. Sci. 583 (2005) 281–296.
[31] J. Jelic, R.J. Meyer, Catal. Today 136 (2008) 76–83.
[32] G. Kresse, J. Furthmuller, Phys. Rev. B 54 (1996) 11169–11186.
[33] G. Kresse, J. Furthmuller, Comput. Mater. Sci. 6 (1996) 15–50.
[34] D. Vanderbilt, Phys. Rev. B 41 (1990) 7892–7895.
[35] J.P. Perdew, Y. Wang, Phys. Rev. B 45 (1992) 13244–13249.
[36] H.J. Monkhorst, J.D. Pack, Phys. Rev. B 13 (1976) 5188–5192.
[37] G. Henkelman, B.P. Uberuaga, H. Jonsson, J. Chem. Phys. 113 (2000) 9901–9904.
[38] A.A. Gokhale, J.A. Dumesic, M. Mavrikakis, J. Am. Chem. Soc. 130 (2008) 1402–1414.
[39] P. Liu, J.A. Rodriguez, J. Chem. Phys. 126 (2007) 164705.
[40] Y. Chen, J. Cheng, P. Hu, H.F. Wang, Surf. Sci. 602 (2008) 2828–2834.
[41] S.D. Senanayake, D. Stacchiola, P. Liu, C.B. Mullins, J. Hrbek, J.A. Rodriguez, J. Phys. Chem. C 113 (2009) 19536–19544.
[42] R. Burch, Phys. Chem. Chem. Phys. 8 (2006) 5483–5500.
[43] F.C. Meunier, D. Tibiletti, A. Goguet, S. Shekhtman, C. Hardacre, R. Burch, Catal. Today 126 (2007) 143–147.
[44] D. Tibiletti, F.C. Meunier, A. Goguet, D. Reid, R. Burch, M. Boaro, M. Vicario, A. Trovarelli, J. Catal. 244 (2006) 183–191.
[45] S. Hilaire, X. Wang, T. Luo, R.J. Gorte, J. Wagner, Appl. Catal. A 215 (2001) 271–278.
[46] T. Shido, Y. Iwasawa, J. Catal. 141 (1993) 71–81.
[47] G. Jacobs, E. Chenu, P.M. Patterson, L. Williams, D. Sparks, G. Thomas, B.H. Davis, Appl. Catal. A 258 (2004) 203–214.
[48] M.M. Schubert, H.A. Gasteiger, R.J. Behm, J. Catal. 172 (1997) 256–258.
[49] L.C. Grabow, A.A. Gokhale, S.T. Evans, J.A. Dumesic, M. Mavrikakis, J. Phys. Chem. C 112 (2008) 4608–4617.
[50] P.J. Feibelman, B. Hammer, J.K. Norskov, F. Wagner, M. Scheffler, R. Stumpf, R. Watwe, J. Dumesic, J. Phys. Chem. B 105 (2001) 4018–4025.

[51] M. Mavrikakis, B. Hammer, J.K. Norskov, Phys. Rev. Lett. 81 (1998) 2819–2822.
[52] B. Hammer, O.H. Nielsen, J.K. Norskov, Catal. Lett. 46 (1997) 31–35.
[53] M.G. Evans, M.P. Polanyi, Chem. Soc. Faraday Trans. 34 (1938) 11–24.
[54] J.K. Norskov, T. Bligaard, A. Logadottir, S. Bahn, L.B. Hansen, M. Bollinger, H. Bengaard, B. Hammer, Z. Sljivancanin, M. Mavrikakis, Y. Xu, S. Dahl, C.J.H. Jacobsen, J. Catal. 209 (2002) 275–278.
[55] A. Michaelides, Z.P. Liu, C.J. Zhang, A. Alavi, D.A. King, P. Hu, J. Am. Chem. Soc. 125 (2003) 3704–3705.
[56] T. Bligaard, J.K. Norskov, S. Dahl, J. Matthiesen, C.H. Christensen, J. Sehested, J. Catal. 224 (2004) 206–217.
[57] N. Bronsted, Chem. Rev. 5 (1928) 231–338.
[58] A.A. Phatak, W.N. Delgass, F.H. Ribeiro, W.F. Schneider, J. Phys. Chem. C 113 (2009) 7269–7276.
[59] J. Nakamura, J.M. Campbell, C.T. Campbell, J. Chem. Soc. Faraday Trans. 86 (1990) 2725–2734.
[60] N. Guo, W.D. Williams, B.R. Fingeland, V.F. Kispersky, L. Bollmann, J. Jelic, W.N. Delgass, F.H. Ribeiro, R.J. Meyer, J.T. Miller, Phys. Chem. Chem. Phys., submitted for publication.
[61] J. Bergeld, B. Kasemo, D.V. Chakarov, Surf. Sci. 495 (2001) L815–L820.
[62] P. Koci, F. Plat, J. Stepanek, S. Bartova, M. Marek, M. Kubicek, V. Schmeisser, D. Chatterjee, M. Weibel, Catal. Today 147 (2009) S257–S264.
[63] D. Bhatia, R.D. Clayton, M.P. Harold, V. Balakotaiah, Catal. Today 147 (2009) S250–S256.